Stable Gold Carbene | Hot Paper

DOI: 10.1002/anie.201404032

Isolation of a Non-Heteroatom-Stabilized Gold–Carbene Complex**

*Matthias W. Hussong, Frank Rominger, Petra Krämer, and Bernd F. Straub**

Abstract: *Gold–carbene complexes are essential intermediates in many gold-catalyzed organic-synthetic transformations. While gold–carbene complexes with direct, vinylogous, or phenylogous heteroatom substitution have been synthesized and characterized, the observation in the condensed phase of electronically non-stabilized gold–carbenes has so far remained elusive. The sterically extremely shielded, emerald-green complex $[IPr^{**}Au{=}CMes_2]^+[NTf_2]^-$ has now been synthesized, isolated, and fully characterized. Its absorption maximum at 642 nm, in contrast to 528 nm of the red-purple carbocation $[Mes_2CH]^+$, clearly demonstrates that gold is more than just a "soft proton".*

Gold complexes catalyze the addition of nucleophilic functional groups across C–C triple bonds.[1] The unraveling of reaction mechanisms in homogeneous gold catalysis is of fundamental importance for the rational development of catalyst complexes and synthetic transformations. Thus, the identification and the synthetic, spectroscopic, and computational characterization of highly reactive transient catalyst intermediates such as gold–carbene complexes has been in the focus of ongoing research.[2] Gold carbenes without stabilization by heteroatom substituents are proposed as mandatory intermediates in many catalytic cycles. A controversy has emerged about the electronic character as either carbene-like with significant gold-to-carbon back-bonding[3] or carbenium-like with marginal back-bonding.[4] However, structurally[3–6] or spectroscopically[7–9] characterized gold–carbene complexes that have been reported are comprised either of iminio ylide-type or oxonio ylide-type ligands (Figure 1). The synthesis of non-heteroatom-stabilized gold carbenes has been rated as a formidable challenge: "Back-donation of electron density from gold to the vacant carbene π-orbital" … "alone is evidently too small to impart finite lifetimes onto such species."[6]

Owing to our long-standing interest in d^{10} metal carbene complexes,[10] Weber in our research group synthesized the extremely sterically demanding *N*-heterocyclic carbene ancillary ligand IPr**.[11] It is an octa-*tert*-butyl derivative of Berthon-Gélloz's and Markó's IPr* ligand.[12] The ligand system IPr** has been rationally designed for the isolation and characterization of highly reactive transition-metal complexes. Indeed, IPr**AuCl caught $AgSbF_6$ red-handed in the abstraction of a chloride ligand.[13] An IPr**Au cation without donor-solvent coordination heterolytically cleaves a C–B bond of the $[B\{C_6H_3\text{-}3,5\text{-}(CF_3)_2\}_4]^-$ counterion within days at room temperature.[14] Despite (or rather because of) its steric shielding, IPr**AuNTf$_2$ (**1**) is highly catalytically active in the Hashmi phenol synthesis.[15] In this study, we used a sterically demanding diazomethane substrate as carbene precursor compound, aiming to prepare, isolate, and characterize spectroscopically a "true" gold–carbene complex with high carbenoid character. Indeed, the reaction of red dimesityldiazomethane[16] with colorless IPr**AuNTf$_2$ (**1**)[15] in dichloromethane yields an intensely emerald-green, diamagnetic, and remarkably water-, air-, and thermostable gold–carbene complex nearly quantitatively within hours (Scheme 1).

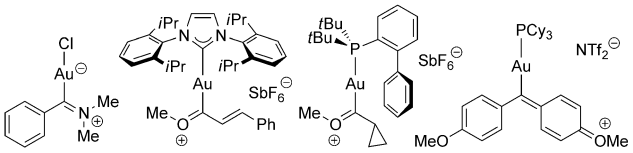

Figure 1. Structurally characterized gold–carbene complexes with prevailing iminio ylide (left),[2a,3] oxonio ylide (center left and center right),[4,5] and phenylogous oxonio ylide ligand character (right).[6]

The gold bistriflimide **1** releases a 12-valence-electron gold cation that coordinates dimesityldiazomethane and

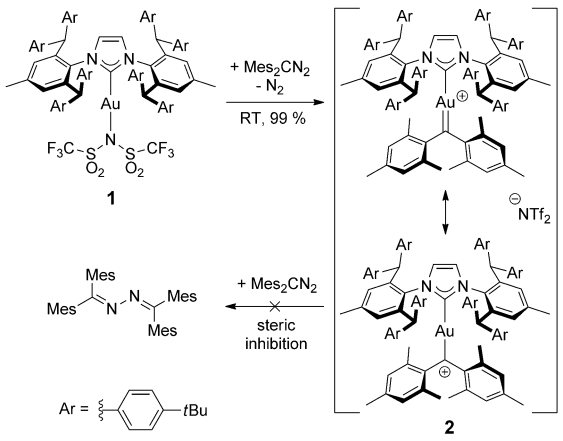

Scheme 1. Synthesis of a gold–carbene without heteroatom stabilization.

[*] M. Sc. M. W. Hussong, Dr. F. Rominger,[+] P. Krämer,[++]
Prof. Dr. B. F. Straub
Organisch-Chemisches Institut, Universität Heidelberg
Im Neuenheimer Feld 270, 69120 Heidelberg (Germany)
E-mail: Straub@oci.uni-heidelberg.de
Homepage: http://www.uni-heidelberg.de/fakultaeten/chemgeo/oci/akstraub

[+] Responsible for the single-crystal X-ray diffraction analysis.

[++] Responsible for IR and UV/Vis measurements.

[**] Financial support by the Universität Heidelberg and the DFG is gratefully acknowledged.

Supporting information for this article is available on the WWW under http://dx.doi.org/10.1002/anie.201404032.

eventually eliminates the ideal leaving group N_2. The key point in the successful preparation of gold–carbene complex **2** is the steric inhibition of the undesired C–N bond formation of the electrophilic carbene ligand with the nucleophilic terminal nitrogen of a second molecule dimesityldiazomethane (Scheme 1, bottom). The extreme steric shielding of the carbene center becomes evident in the ball-and-stick representation of the cationic gold–carbene complex from a single-crystal X-ray diffraction study (Figure 2).

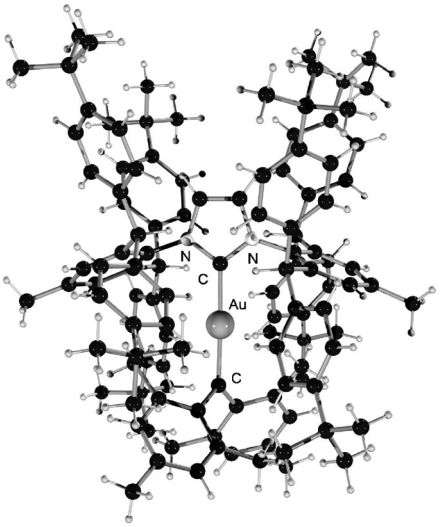

Figure 2. Ball-and-stick model of the gold–carbene cation of salt **2** in the solid state.[17] Bistriflimide counterion and two toluene molecules have been omitted for clarity. Bond lengths: Au–C(IPr**) 203.0(6), Au–$CMes_2$ 201.4(6) pm. Angles: C-Au-C 178.5(2), N-C-Au 127.2(4) and 128.0(4), N-C-N 104.8(5), C(Mes)-C-C(Mes) 116.3(6)°. Angle sum for Au=$CMes_2$ 359.95°.

In the solid-state structure, the mesityl substituents are twisted by $44 \pm 3°$ out of the gold–carbene plane, thereby diminishing the resonance stabilization of the carbene by the aromatic π systems. The Au–$CMes_2$ bond is slightly shorter ($\Delta d_{AuC} = 1.6$ pm) than the Au–C(IPr**) bond. According to Bent's rule,[18] the more electronegative nitrogen atoms in the IPr** ancillary ligand and the larger Au-C-N angles lead to higher carbon s orbital percentage in the Au–C(IPr**) σ bond than in the Au–$CMes_2$ σ bond. Without π back-bonding,[19] the Au–$CMes_2$ bond should have been longer. We attribute the observed overcompensation to a significant, but not predominant double bond character Au=$CMes_2$. This interpretation is in accord with Brooner and Widenhoefer's elegant structural observation of a weak gold-to-carbene back-bonding (Figure 1, center right) that "exceeds that of a methyl or phenyl group".[5]

The $^{13}C\{^1H\}$ NMR spectrum underlines the distinct difference of the iminio ylide-type N-heterocyclic carbene ligand with a chemical shift of $\delta = 185.1$ ppm, and the carbene ligand with a signal at $\delta = 321.3$ ppm (Figure 3). It is even more deshielded than the gold–carbene signal of Aznar at $\delta =$ 281.5 ppm,[4] of Widenhoefer at $\delta = 303.9$ ppm,[5] and of Fürstner at $\delta = 284.5$ ppm (Figure 1, second to fourth structure).[6]

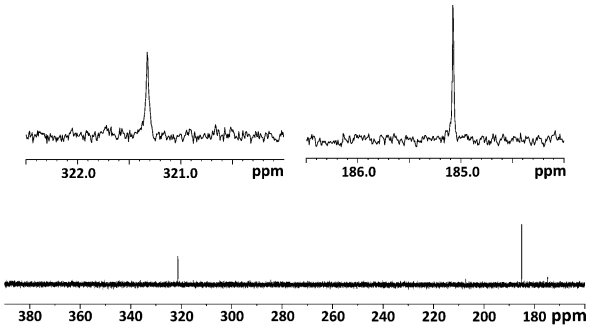

Figure 3. $^{13}C\{^1H\}$ NMR spectrum (150.93 MHz, 298 K, $CDCl_3$) of complex **2**: carbene ligand signal (left) and IPr** iminio ylide ligand signal (right).

In the crystal structure, the *ortho* methyl groups of the mesityl substituents are pairwise diastereotopic. At room temperature, ^1H NMR spectra display only one *ortho* methyl group signal with an intensity of twelve protons, indicating rapid rotation of the mesityl groups. At low temperatures, however, broadening of the signal is observed, leading to two signals below −90 °C (Figure 4, top). A similar behavior

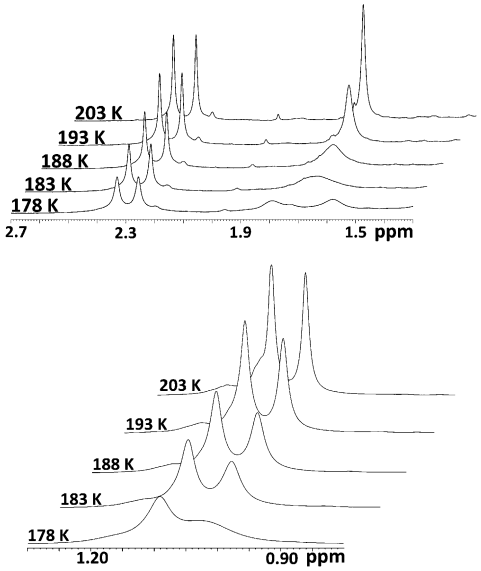

Figure 4. ^1H NMR coalescence of the signals of the diastereotopic *ortho*-methyl groups at −90 °C (top spectrum) and of one of the IPr** *tert*-butyl substituent sets at −95 °C (bottom spectrum) at 300 MHz in CD_2Cl_2.

occurs with a signal at $\delta = 1.19$ ppm (Figure 4, bottom), comprising the 36 protons for the four *tert*-butyl substituents of the IPr** ligand in close proximity to the intrinsically C_2-symmetrical dimesitylcarbene ligand.

The free energy of activation for the concerted mesityl group rotation of approximately 36 ± 2 kJ mol^{-1} stems from both the energetically unfavorable orientation of the two mesityl substituents in the transition state (Scheme 2), and the reorganization of IPr** *tert*-butylphenyl fragments.

The emerald-green color of complex **2** is due to the absorption of violet-blue and red light (Figure 5): absorption

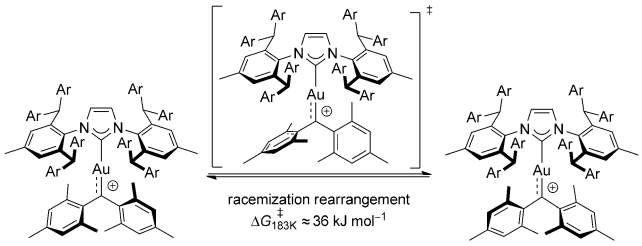

Scheme 2. Rapid degenerate rearrangement of the C_2-symmetrical cationic gold–carbene by concerted rotation of the mesityl substituents.

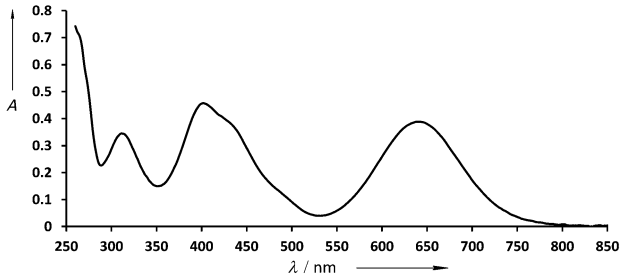

Figure 5. UV/Vis spectrum of gold–carbene **2** in dichloromethane.

bands were observed at 312 nm (log $\varepsilon = 3.8$), 401 nm (log $\varepsilon = 3.9$), 435 nm (log $\varepsilon = 3.8$), 490 nm (log $\varepsilon = 3.4$), and at 642 nm (log $\varepsilon = 3.9$). We have performed TDDFT[20] calculations on an optimized structure of the C_2-symmetric 1,3-dimethylimidazol-2-ylidene gold–dimesitylcarbene cation in the gas phase at the M06/LACV3P** ++ level of theory,[21] as implemented in the jaguar program package.[22] The observed 642 nm absorption maximum essentially corresponds to the electronic transition from the HOMO, which is based on an antibonding σ interaction of an sp^2-hybridized singlet carbene with a gold 5d orbital, into the LUMO, which is dominated by the empty p orbital of the carbene (Scheme 3).

Apart from comparison of structural parameters, such as C–C and Au=C versus Au–C bond lengths, the bathochromic red-shift is a superb measure of the electronic classification as gold–carbene complexes with high carbenoid character, in contrast to complexes with predominant iminio ylide or oxonio ylide ligand character.

The bathochromic shift by formal replacement of the benzhydrylic proton in red-purple $[Mes_2CH]^+[HSO_4]^-$ ($\lambda_{max} = 528$ nm, Figure 6 left)[23] by IPr**Au$^+$ to the emerald-green carbene complex **2** (Figure 6, right) literally shows that gold(I) fragments are more than just "soft protons". Thus, a dualistic discussion about "carbene" character (Au=C bond order of 2) versus "carbenium" character (Au–C bond order of 1) is incomplete. A carbenoid resonance structure with a gold–carbon bond order of zero must be considered as third relevant electronic contribution (Scheme 4). The antibonding interaction of the gold $5d^{10}$ shell with the sp^2 donor-electron pair of the carbene ligand (HOMO in Scheme 3) weakens the σ bond of gold–carbenes, being a major cause for the kinetic and thermodynamic lability of the gold–carbene moiety. As a rule of thumb, weak metal–carbene bonds lead to the

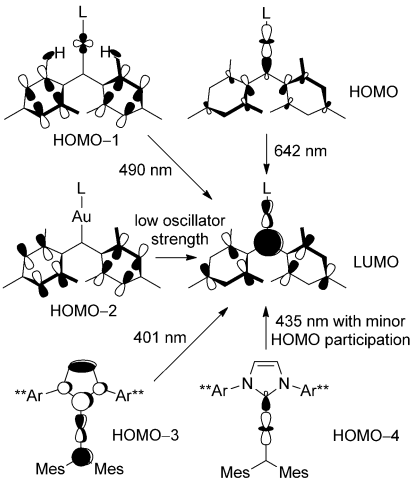

Scheme 3. Assignment of observed absorption bands and representation of the electronic transitions from occupied molecular orbitals to the lowest unoccupied molecular orbital in gold–carbene complex **2**.

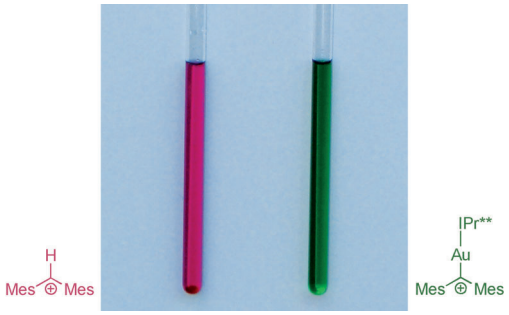

Figure 6. Solutions of red-purple $[Mes_2CH]^+[HSO_4]^-$ (left) and of the emerald-green gold–carbene complex **2** (right) in CH_2Cl_2.

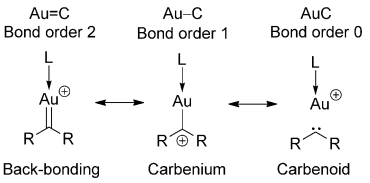

Scheme 4. Au–C bond orders of gold–carbene resonance structures.

cyclopropanation of alkene substrates, while strong metal–carbene bonds favor alkene metathesis reactions. The UV/Vis data of complex **2** supports Toste's quantum-chemical conclusion that the overall bond order of gold–carbenes is "generally less than or equal to one".[24] The contribution of a third resonance structure with an AuC bond order of zero resolves the paradox of bond orders of less than one based on resonance structures with higher bond orders of one and two.

In summary, we have synthesized and fully characterized a non-heteroatom-stabilized gold–carbene complex with predominant carbenium character. The solid-state structure corroborates a minor contribution of an Au=C double-bond

resonance structure. The UV/Vis absorption spectrum underlines the essential role of the antibonding interaction of the filled gold $5d^{10}$ shell with the carbene ligand sp^2 donor-electron pair, resulting in a thermodynamically weak gold–carbene bond. As a consequence, the conceptual limits of the isolobal designation of gold as a "soft proton" should be acknowledged. With these results at hand, the detection and even isolation of highly reactive gold–carbene complexes with even more pronounced gold–carbene back-bonding and an even larger bathochromic shift seems possible, opening the path for direct investigations in the condensed phase of proposed intermediary carbene species in homogeneous gold catalysis.

Received: April 5, 2014
Published online: June 20, 2014

Keywords: bond order · carbenes · gold · homogeneous catalysis · intermediates

[1] For reviews, see: a) D. J. Gorin, F. D. Toste, *Nature* **2007**, *446*, 395 – 403; b) A. Fürstner, *Acc. Chem. Res.* **2014**, *47*, 925 – 938; c) C. Obradors, A. M. Echavarren, *Chem. Commun.* **2014**, *50*, 16 – 28; d) A. Fürstner, P. W. Davies, *Angew. Chem.* **2007**, *119*, 3478 – 3519; *Angew. Chem. Int. Ed.* **2007**, *46*, 3410 – 3449; e) A. Fürstner, *Chem. Soc. Rev.* **2009**, *38*, 3208 – 3221; f) M. Rudolph, A. S. K. Hashmi, *Chem. Soc. Rev.* **2012**, *41*, 2448 – 2462.

[2] a) G. Seidel, B. Gabor, R. Goddard, B. Heggen, W. Thiel, A. Fürstner, *Angew. Chem.* **2014**, *126*, 898 – 901; *Angew. Chem. Int. Ed.* **2014**, *53*, 879 – 882; b) A. S. K. Hashmi, *Angew. Chem.* **2008**, *120*, 6856 – 6858; *Angew. Chem. Int. Ed.* **2008**, *47*, 6754 – 6756; c) A. S. K. Hashmi, *Angew. Chem.* **2010**, *122*, 5360 – 5369; *Angew. Chem. Int. Ed.* **2010**, *49*, 5232 – 5241; d) L.-P. Liu, G. B. Hammond, *Chem. Soc. Rev.* **2012**, *41*, 3129 – 3139; e) H. G. Raubenheimer, H. Schmidbaur, *S. Afr. J. Sci.* **2011**, *107*, 31 – 43.

[3] U. Schubert, K. Ackermann, R. Aumann, *Cryst. Struct. Comm.* **1982**, *11*, 591 – 594.

[4] M. Fañanás-Mastral, F. Aznar, *Organometallics* **2009**, *28*, 666 – 668.

[5] R. E. M. Brooner, R. A. Widenhoefer, *Chem. Commun.* **2014**, *50*, 2420 – 2423.

[6] G. Seidel, A. Fürstner, *Angew. Chem.* **2014**, *126*, 4907 – 4911; *Angew. Chem. Int. Ed.* **2014**, *53*, 4807 – 4811.

[7] M. M. Hansmann, F. Rominger, A. S. K. Hashmi, *Chem. Sci.* **2013**, *4*, 1552 – 1559.

[8] Y. Shi, K. E. Roth, S. D. Ramgren, S. A. Blum, *J. Am. Chem. Soc.* **2009**, *131*, 18022 – 18023.

[9] D. H. Ringger, P. Chen, *Angew. Chem.* **2013**, *125*, 4784 – 4787; *Angew. Chem. Int. Ed.* **2013**, *52*, 4686 – 4689.

[10] B. F. Straub, P. Hofmann, *Angew. Chem.* **2001**, *113*, 1328 – 1330; *Angew. Chem. Int. Ed.* **2001**, *40*, 1288 – 1290.

[11] S. G. Weber, C. Loos, F. Rominger, B. F. Straub, *ARKIVOC* **2012**, 226 – 242.

[12] G. Berthon-Gélloz, M. A. Siegler, A. L. Spek, B. Tinant, J. N. H. Reek, I. E. Markó, *Dalton Trans.* **2010**, *39*, 1444 – 1446.

[13] S. G. Weber, F. Rominger, B. F. Straub, *Eur. J. Inorg. Chem.* **2012**, 2863 – 2867.

[14] S. G. Weber, D. Zahner, F. Rominger, B. F. Straub, *Chem. Commun.* **2012**, *48*, 11325 – 11327.

[15] S. G. Weber, D. Zahner, F. Rominger, B. F. Straub, *ChemCatChem* **2013**, *5*, 2330 – 2335.

[16] H. E. Zimmermann, D. H. Paskovich, *J. Am. Chem. Soc.* **1964**, *86*, 2149 – 2160.

[17] CCDC 994932 contains the supplementary crystallographic data for this paper. These data can be obtained free of charge from The Cambridge Crystallographic Data Centre via www.ccdc.cam.ac.uk/data_request/cif. a) L. J. Farrugia, *J. Appl. Crystallogr.* **1997**, *30*, 565; b) Persistence of Vision Ray Tracer (POV-Ray), http://www.povray.org.

[18] H. A. Bent, *Chem. Rev.* **1961**, *61*, 275 – 311.

[19] a) M. J. S. Dewar, *Bull. Soc. Chim. Fr.* **1951**, *18*, C71 – C79; b) J. Chatt, L. A. Duncanson, *J. Chem. Soc.* **1953**, 2939 – 2942.

[20] E. Runge, E. K. U. Gross, *Phys. Rev. Lett.* **1984**, *52*, 997 – 1000.

[21] a) Y. Zhao, D. G. Truhlar, *Theor. Chem. Acc.* **2008**, *120*, 215 – 241; b) R. Krishnan, J. S. Binkley, R. Seeger, J. A. Pople, *J. Chem. Phys.* **1980**, *72*, 650 – 654; c) P. J. Hay, W. R. Wadt, *J. Chem. Phys.* **1985**, *82*, 299 – 310.

[22] *Jaguar*, version 7.9, Schrodinger, LLC, New York, NY, **2011**.

[23] A. F. Hegarty, V. E. Wolfe, *ARKIVOC* **2008**, 161 – 182.

[24] D. Benitez, N. D. Shapiro, E. Tkatchouk, Y. Wang, W. A. Goddard, F. D. Toste, *Nat. Chem.* **2009**, *1*, 482 – 486.

